

ISAE SUPAERO
INSTITUT SUPÉRIEURE DE L'AÉRONAUTIQUE ET DE
L'ESPACE

Designing the new Ozone kite for the 2028 Olympic Games

Romain Lambert

Internship Report

Author : Romain Lambert

Supervisor : Dominik Zimmerman



January, 2025

Contents

List of Figures

Chapter 1

Introduction

1.1 Ozone Kitesurf

Ozone is one of the world's leading manufacturers of Kites and Paragliders, created around a dedicated team of passionate riders and pilots that share the same outstanding passion for nature, exciting sports and progress.

Their products conjure an experience that is nearly impossible to put into words. Invoking emotion, excitement, exhilaration and joy, the Ozone 'feeling' is something that transcends the product itself.

The Ozone factory in Vietnam is a state of the art facility where they employ only the highest trained craftsman whose expertise and attention to detail shine through in every product that is manufactured. their factory produces exclusively for Ozone Kites, Ozone Paragliders, Ozone Speedwings and Squirrel Wingsuits.

All Ozone products are checked and batch tested throughout the manufacturing process and must pass final checks before they leave the factory. Close contact



Figure 1.1: Two Ozone racing kites

between their product development teams and production facility ensures that every product is manufactured to specifications and is guaranteed to be worthy of the Ozone name.

They do not produce in large batches; all products are manufactured to order using their bespoke B2B ordering system. This method of production is unique to the Kitesurf industry, and means there is no extra stock flooding into the market, which can devalue a product at the end of the season.

Since the development of their very first kite in 2001, Ozone has brought more innovative concepts and industry leading designs to market than any other brand while creating category-defining products that set the standard for all those that follow.

They believe strongly in investing in tools that allow their team to advance designs with high efficiency and accuracy. They have developed their own proprietary software OzCAD by collaborating with some of the most brilliant minds in the fields of engineering, aerodynamics and software development.

Ozone has created the Version Concept for all products rather than confining them to model years. Designs are updated to a new version when they believe they have developed a better performing product from the existing design.

They have adopted this approach to avoid confusion in model updates; this also gives their design team time for true innovation [?].

1.2 The Ozone design team



Figure 1.2: The Ozone design team involved in this internship

Ozone provided me with the opportunity to work with a myriad of highly skilled and passionate kitesurfing professionals.

The kite design team is composed of :

- **Dominik Zimmermann** : head designer and foil tester
- **Rob Whittall** : product designer, co owner and co founder of Ozone and ex-world paragliding and hang gliding champion
- **Simon Burner** : assistant designer and test rider
- **Torrin Bright** : product manager and test rider

Additionally, throughout the internship, I had frequent interactions with the Ozone paraglider design team. Due to the significant overlap in aerodynamics between these two fields, I was able to leverage their expertise and experience. **Luc Armand** and **Fred Pieri**, research and development engineers and experienced pilots, provided valuable support for my research efforts in developing a Python-based optimization algorithm for their upcoming paraglider design.

Furthermore, **Axel Mazella**, a member of the racing team, two-time Kitefoil World Champion and European Champion, provided me with valuable feedback and insights from his testing of our prototypes. This input helped me better understand the optimization challenges in kite design and bridge the gap between the scientific aspects and the practical realities of kite riding.

1.3 The Olympic Games

The 2024 Olympic Games will introduce kitesurfing for the first time, encompassing various disciplines.

As the name implies, athletes are propelled across the water's surface while holding a 7-21m kite to harness the power of the wind.

In many respects, it represents a fusion of water sports. Competitors need the balance of a surfer while reaching speeds similar to those in windsurfing, using equipment that closely resembles a wakeboard.

When the wind is strong enough, riders can achieve speeds of up to 40 knots (74 km/h) and have been observed soaring up to six meters in the air [?].

Races are typically conducted as short-course, windward-leeward races. The number of races, race format, and course length may vary depending on the event and conditions. They begin with a starting sequence involving flags, signals, and countdowns then, the athletes must reach buoys to complete the race.

The class features a foil kite and a board with a hydrofoil. The equipment is not one-design, but instead competitors use their choice of approved production equipment. The International Kiteboarding Association (IKA) manages the class [?].



Figure 1.3: Example of a trajectory followed during a kite race.

1.4 The Ozone R1V4 formula kite

The current formula kite used by Ozone in the Olympic Games is the R1V4.

However, it faces stiff competition from a more efficient rival, the Flysurfer "VMG". This was the primary objective of the internship: to develop the fifth iteration of the R1 kite, known as the "R1V5," in preparation for the 2028 Olympic Games.

With the registration deadline set for March 2024, there was a very real time constraint in the design of the kite..



Figure 1.4: The Ozone R1V4 formula kite

Chapter 2

2D steady simulations

The initial goal was to identify the factors that contribute to the VMG's superior efficiency compared to the R1V4 and make the necessary adjustments.

The first step involved identifying the parameters that respond to various flight conditions. Following that, a low-fidelity approach using XFLR5 was employed to compute the 2D aerodynamic coefficients, providing insights into the disparities between the airfoils. Subsequently, Fluent CFD software was utilized to obtain a more precise assessment of the aerodynamic coefficients for each airfoil during actual flight conditions.

2.1 Kite flight modelling

The kite is modelized according to the "zero mass model" as developed in the course given by Richard Leloup in Supaero [?].

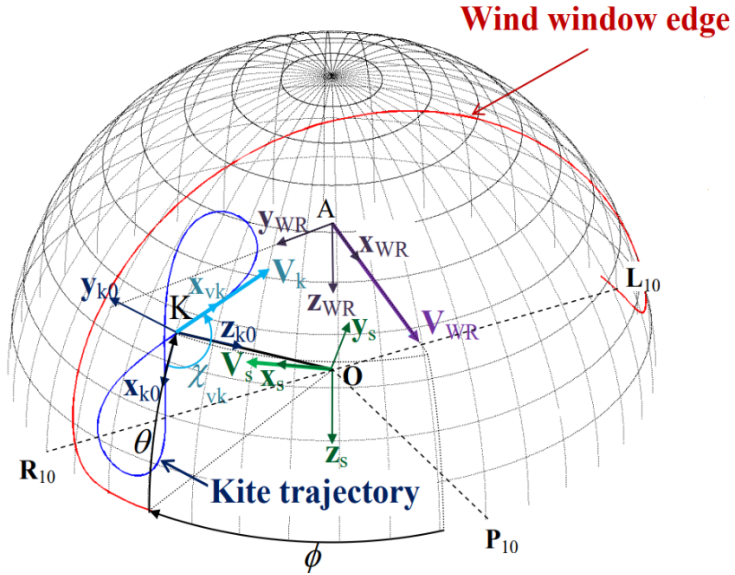


Figure 2.1: Speeds & angles decomposition

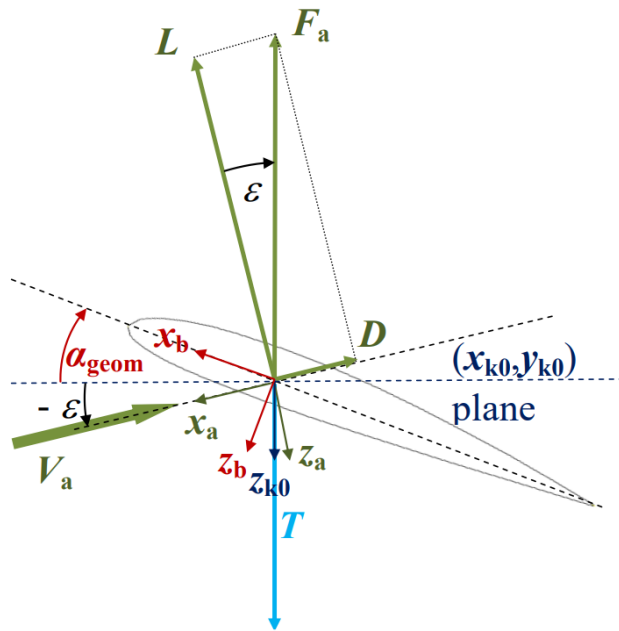


Figure 2.2: Decomposition of the aerodynamic force vector

The Zero-mass model approach leads to the following results :

$$\begin{cases} V_{WR} = V_{WT} - V_S \\ V_a = V_{WR} - V_k \\ F_a = -T = \frac{1}{2} C_L \rho A V_a^2 \end{cases} \quad (2.1)$$

with, in our case of study, $V_k = 0$. As a matter of fact, we are assuming that the kite is static in relation to the ship (the rider).

Then, we can deduce from the relation ?? :

$$\begin{cases} V_a &= \sqrt{V_{WT}^2 + V_s^2 - 2V_{WT}V_s \cos(\alpha_{S,WT})} \\ \epsilon &= \alpha_{S,WT} - \alpha_{a,WT} \\ \alpha_{a,WT} &= \arctan\left(\frac{V_s \sin(\alpha_{S,WT})}{V_s \cos(\alpha_{S,WT}) - V_{WT}}\right) \end{cases} \quad (2.2)$$

Then, we understand that depending on the position of the kite (Φ, Θ), the rider's speed (V_s) and the true wind speed (V_{WT}), the tether tension (T) is very different. This result has lead to the definition of the wind window represented on the figure ??.

The concept of the wind window holds significant importance in kitesurfing as it presents riders with a fundamental trade-off: the closer the kite is positioned to the center of the wind window, the more power it generates. However, this ideal kite placement might not align with the rider's intended direction. As a result, kitesurfers must strategically position their kites within the wind window to maximize power in their desired direction.

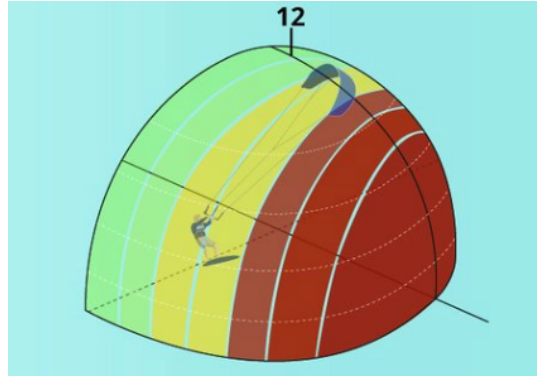


Figure 2.3: The wind window

2.2 The different phases

A kite race is segmented into distinct phases, each corresponding to varying inlet conditions. What's of primary importance for the riders during these phases is their "Velocity Made Good," often referred to as VMG, which signifies their speed aligned with the axis they intend to follow (the wind axis).

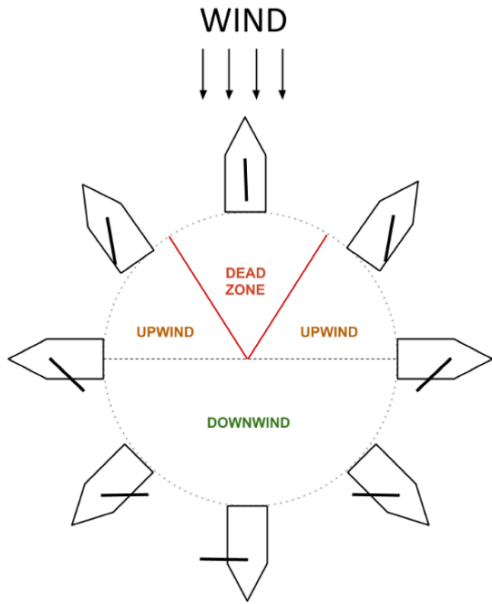


Figure 2.4: Upwind and downwind diagram

2.2.1 The upwind

Advancing upwind involves traveling in the direction opposite to the wind. This segment typically accounts for approximately $\frac{2}{5}$ of the entire race.

In this phase, the kite operates at lower angles of attack, resulting in its highest relative speed. Riders in this phase aim to strike a balance between gripping the bar for increased power, which can cause the kite to shift back within the wind window, and releasing the bar for reduced tether tension, allowing the kite to move toward the edge of the wind window.

2.2.2 The downwind

Heading downwind involves traveling in the same direction as the wind. This phase typically constitutes about $\frac{3}{5}$ of the entire race duration. In this stage, the kite operates with steep angles of attack, resulting in its slowest relative speed.

As a consequence, the rider must maintain a firmer grip on the bar to increase their VMG (enabling them to head as far downwind as possible). However, they also need to release the bar at times, allowing the kite to move freely, in order to increase tether tension – the opposite of what's done during the upwind phase. In this phase, maintaining tension in the lines proves to be particularly challenging due to the slower relative speed. Additionally, a larger kite provides the rider with more power during this phase.

2.2.3 The transition

The transition is the moment when the rider changes direction (tacks or jibes). At this moment, the rider doesn't want the kite to lift him out of the water, or he would lose his balance and fall.

2.2.4 The crosswind

This phase represents around $\frac{1}{5}$ of the entire race. It has not been considered in this study as it relies on the upwind and downwind performances.

2.3 Experimental data

Ozone benefits from working with world-renowned kiters, also known as "team riders". Axel Mazella, two times Kitefoil World Champion (2017 and 2019) and European Champion (2019), is a racing team rider and tester for Ozone. Thanks to him, I have had access to his Palma racing (29/04/2023) data that are a "good reference" for understanding speeds and angles that are to be considered in a formula kite race.

The following table ?? gives the average values from this very race :

	$\alpha_{s,WT}(\circ)$	$V_{WT}(knots)$	$V_S(knots)$
Upwind	39,5	14,0	22,5
Downwind	155,0	14,0	31,5

Table 2.1: Average data from Axel's race

From these values and according to the equation ??, we can deduce (??):

	$\epsilon(\circ)$	$V_a(knots)$
Upwind	15,0	34,5
Downwind	15,0	20,5

Table 2.2: Average ϵ and V_a from Axel's race

Nonetheless, these ϵ values appear impractical as they would imply angles of attack exceeding 15° , which is excessively high.

Conversations with the Ozone team and other kitesurfing experts, including individuals like Benoît Augier, a researcher specializing in fluid mechanics at the Marine Hydrodynamics Laboratory in Brest, who closely collaborates with the French Kitesurfing team for the Olympic Games, revealed that these ϵ values are notably distant from reality. In fact, they represent a realm of calculations that has yet to be theoretically determined and prove challenging to measure through experimental means.

As a matter of fact, The previous results assume a 90° angle between the rider and his lines. However, as shown in ??, the position of the kite in the wind window and the position of the bar (handled by the rider) constantly change while kitesurfing and greatly modify the value of α_i . Moreover, the link between the lift and the tether tension from ?? is changed if we considered the lines to make an angle δ with the athlete.

Nevertheless, considering the physical limitations and the aerodynamic flight equations of a kite, it is possible to derive the following outcomes :

$$\left\{ \begin{array}{l} \delta \in [0, \epsilon] \\ T \cos(\delta) = L \cos(\epsilon) \\ a_{geom} + \epsilon - \delta = \alpha_i \end{array} \right. \quad (2.3)$$

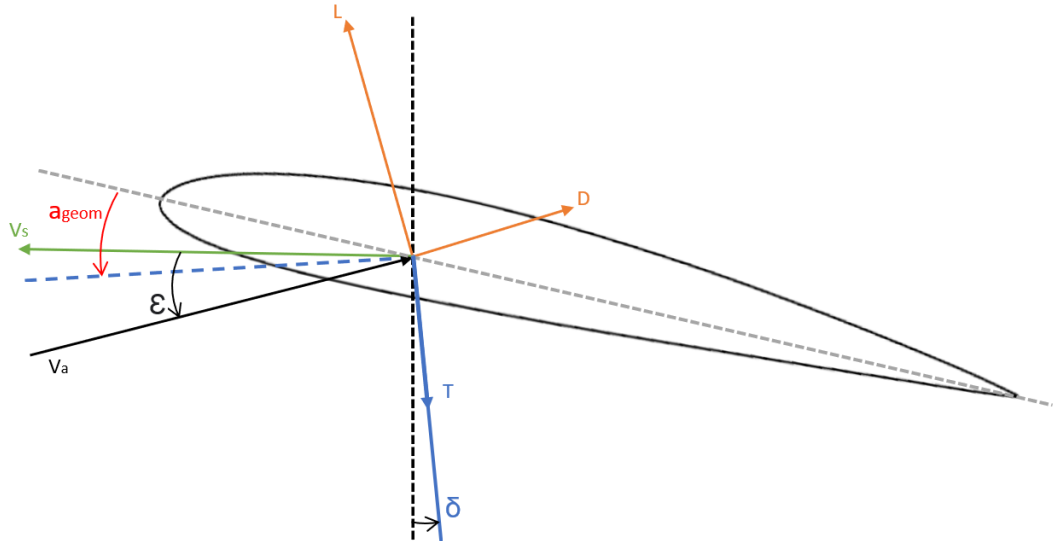


Figure 2.5: Angle decomposition, taking into account the angle δ between the lines and the athlete

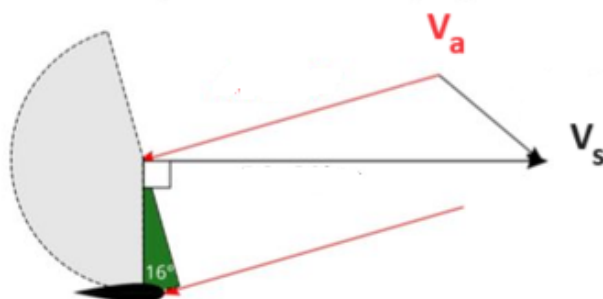


Figure 2.6: The range of possible values for δ with an angle between the athlete's velocity vector and the apparent wind of 16°

Consequently, the table ?? presents the generally acknowledged input parameters for a kite, as per the insights of kitesurfing experts and in consideration of Axel's race data :

	$\alpha_i(^{\circ})$	$V_a(knots)$
Upwind	0 - 5	30 - 35
Downwind	7 - 14	18 - 23

Table 2.3: Commonly accepted inlet values

2.4 XFLR5 - The plot of the aerodynamic polars

2.4.1 XFLR5

XFLR5 is an analysis tool for airfoils, wings and planes operating at low Reynolds Numbers.

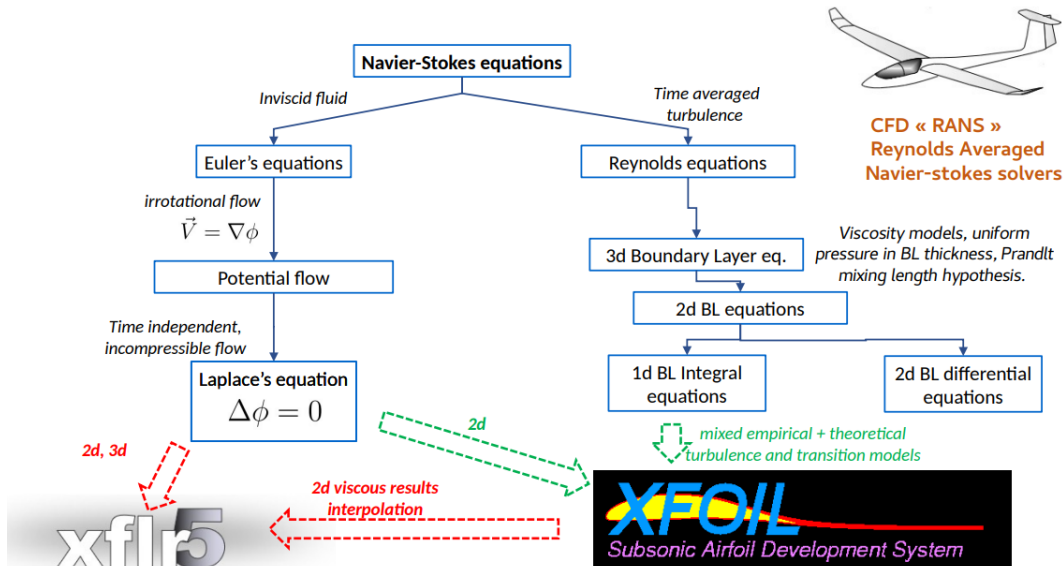


Figure 2.7: XFLR5 theory diagram

XFLR5 uses the "simultaneous" scheme, Developed by M. Drela and H. Youngren in the 1990s (XFOIL) at MIT, for solving the interactive boundary layer problem. It means that the inviscid and boundary layer equations are solved concurrently at each iteration[?].

In 2d, XFOIL implements a full interactive boundary layer loop. However, XFOIL ultimately yields results that are accurate within the linear angle of attack range and below a Mach number of 0.4 but tends to overpredict lift and underpredict drag unless the flow is in the compressible regime. XFOIL cannot accurately model stall and post-stall conditions due to the nature of the solver[?].

2.4.2 The polars

Using XFLR5, I was able to plot the polars of the "R1 V4", the current Ozone kite, the "R1 V5", the next version of the R1 kites and the "VMG", the current kite of Flysurfer that was to be outperformed.

The upwind polars have been plotted using a speed of 35 knots and a Reynolds number of $1,3e^6$

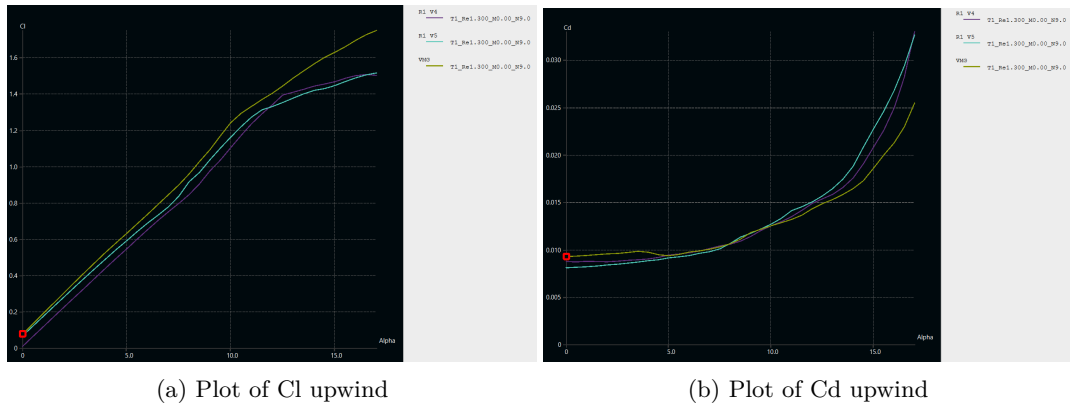


Figure 2.8: Upwind plots

These polars are interesting for low angles of attack ($0\text{--}5^\circ$ according to ??) where one can see that the VMG and R1 V5 have a higher C_l than the R1 V4 and the R1 V5 has a lower C_d than the R1 V4 and the VMG.

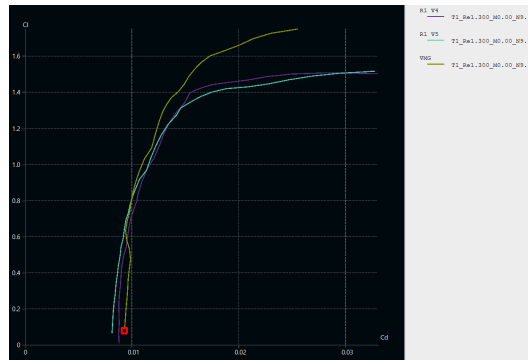


Figure 2.9: Upwind polars

Moreover, according to the team rider Axel Mazzella, "the R1 V4 is the one that does not fly enough to the edge of the wind window when the rider slacks (going upwind)". The lack of C_l (and therefore of finesse) in these conditions may be an explanation to that phenomena.

However, these results need to be nuanced by the fact that at this stage the 3d effects are not taken into account.

For all the airfoils, the boundary layer transition from laminar to turbulent appears around 20% of the chord on the upper surface and 70% on the lower surface

at an angle of attack of 5° . However, this result should be nuanced by the presence of seams along the leading edge of the kite, likely causing an earlier transition. Later in the internship, the transition had been deliberately induced to occur at the leading edge, and the comparison between the kites remained consistent.

Then, the downwind polars have been plotted using a speed of 20 knots and a Reynolds number of $0,7e^6$

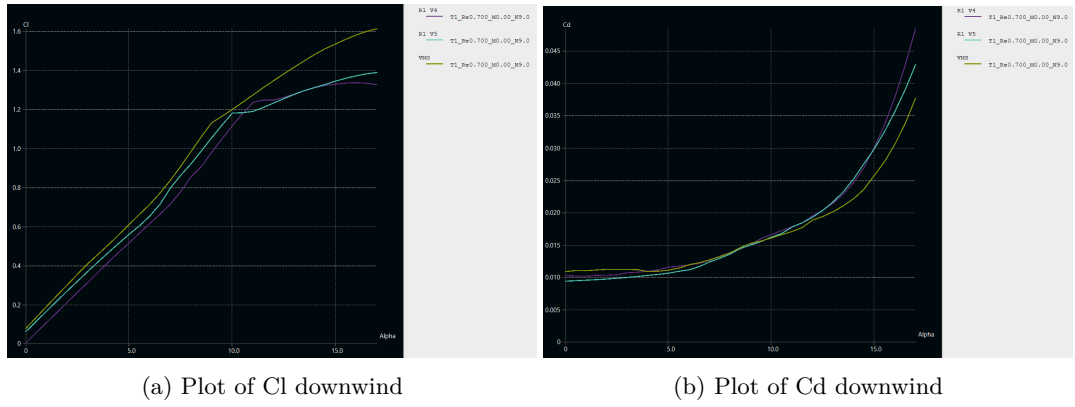


Figure 2.10: Downwind plots

These polars are interesting for higher angles of attack ($7\text{-}14^\circ$ according to ??) and need to be nuanced by the low reliability of XFLR5 at high angles of attack (near the stall and post-stall) [?].

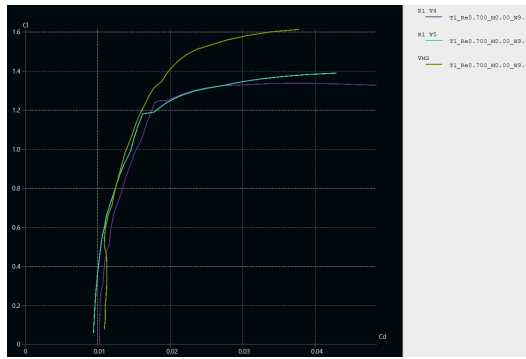


Figure 2.11: Downwind polars

We can see from these polars that the VMG has a higher C_l than the R1s and a lower C_d .

According to Axel "the main issue with the R1 V5 is the low tether tension during this phase that can lead to a loose of tensions in the lines and its difficulty to fly forward when hauling the bar".

Furthermore, comparing the R1 V4, which was only tested with three line sets, to the R1 V5 and the VMG, both of which were tested with only two line sets,

proves challenging. In fact, Axel's observation suggests that with three lines, "the kite's shape is reinforced, and it catches the wind more quickly, resulting in a shorter transition time."

From this, it becomes apparent that the disparities in performance between the kites cannot be solely attributed to the airfoil design. Other factors, such as 3D effects and the number of lines, could provide a more comprehensive explanation for these results.

For all the airfoils, the boundary layer transition from laminar to turbulent appears around 16-19% of the chord on the upper surface and does not transit on the lower surface at an angle of attack of 10°.

From these results, and in connection with the experience of the team rider and both Ozone design teams (paraglider and kite), it appears that increasing the aerodynamic finesse of the R1 and enhancing lift in downwind conditions would enable them to surpass the VMG.

2.5 The airfoil design

Based on the preceding findings and in consultation with the Ozone design team, we generated the following Cp plot and conducted a comparative analysis of the foil designs in order to formulate our approach for the next airfoil prototype to be tested.

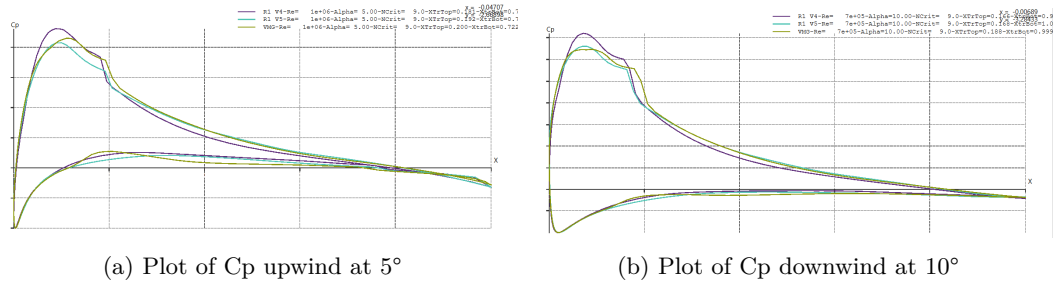


Figure 2.12: Cp plots

We can see in the Cp plots that all kites have a peak of C_p on the upper surface near 10% of the chord then a boundary layer transition near 20% of the chord. However, if the R1 V4 has the highest peak, it also have a higher C_p on the lower surface which leads to a lower C_L . The R1 V5 has a lower C_p peak on the upper surface than the R1 V4 but also a lower C_p on the lower surface.

The VMG upper surface seems to be a good compromise between the three different Cp plot as its peak is lower than the R1 V4 but its turbulent part is higher.

However, the R1s' lower surfaces seem to be better than the VMG because they lead to mostly lower and smoother Cp plot.

If we consider the airfoils, we can see that the VMG lower surface reaches its lowest point earlier than the other airfoils which may lead to a smoother interaction between the intrados and extrados flows at the trailing edge (because its recompression zone is larger).

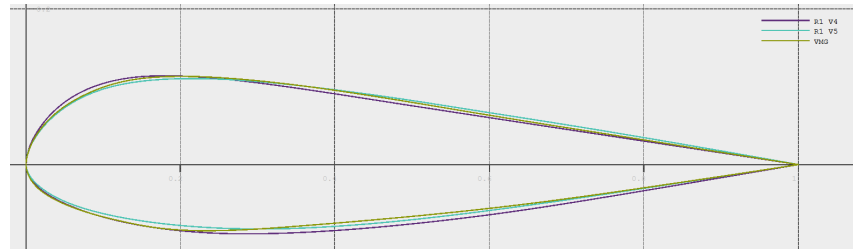
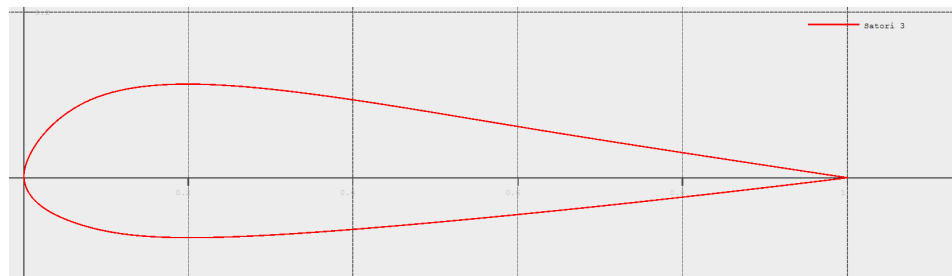
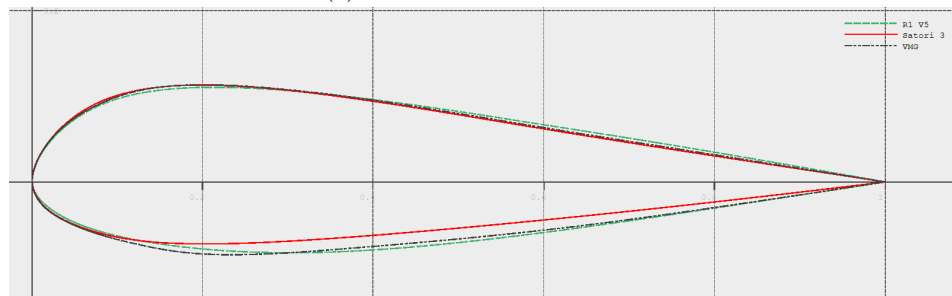


Figure 2.13: The 3 different airfoil designs

As a result, with the help of Rob Whittall, product designer, co-owner and co-founder of Ozone, we designed a new airfoil making the lower surface of the R1 V5 "smoother" and changing the VMG upper surface making its leading edge "rounder". The resulting airfoil was named "R1 V5 Satori 3".



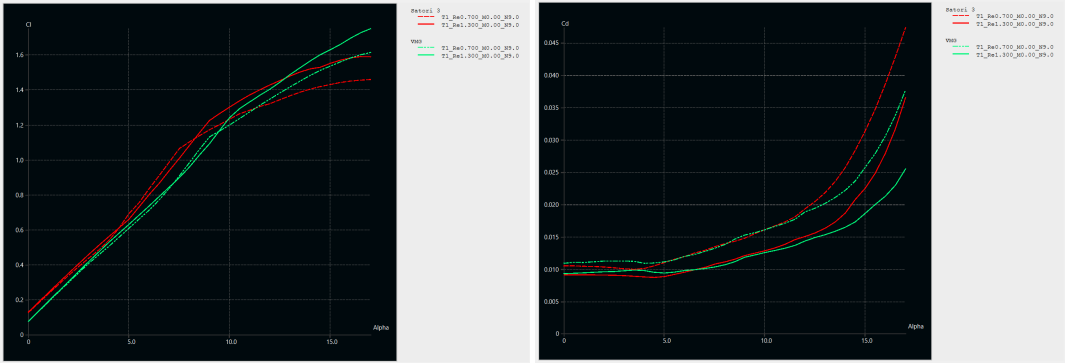
(a) The R1 V5 Satori 3 airfoil



(b) The R1 V5 Satori 3, R1 V5 and VMG airfoils

Figure 2.14: Cp plots

The following graphs ?? and ?? show that the R1 V5 Satori 3 has a higher C_l , lower C_d and, as a result, a higher finesse upwind at 5° and downwind at 10° .



(a) Cl plot

(b) Cd

Figure 2.15: Cd & Cl plots (VMG and R1 V5 Satori 3)

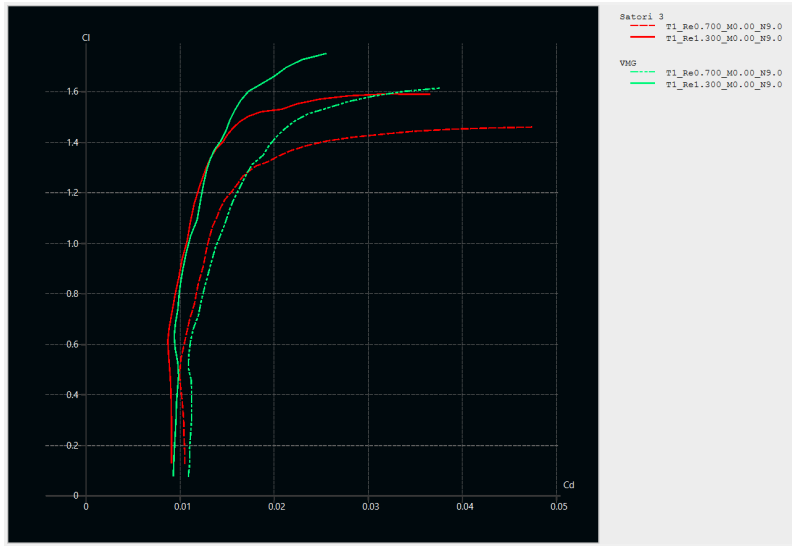
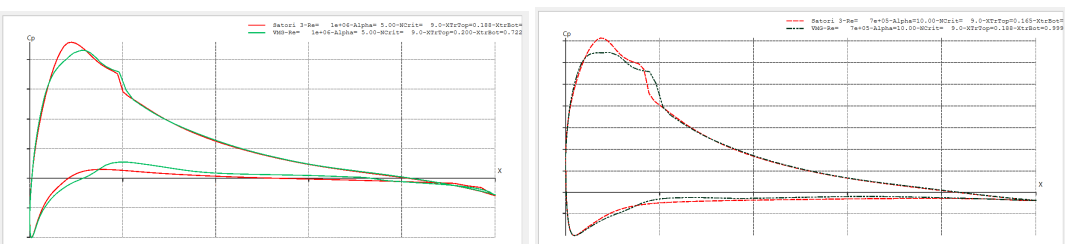


Figure 2.16: Polars (VMG and R1 V5 Satori 3)

Moreover, we can see on the figure ?? that the objectives in term of Cp plot have been reached.



(a) Cp plot upwind at 5°

(b) Cp plot downwind at 10°

Figure 2.17: Cp plots of VMG and R1 V5 Satori 3

2.6 FLUENT - The 2D steady simulations

2.6.1 The spatial convergence

We conducted comparisons using ANSYS FLUENT to refine the results. The objective was to provide Ozone with a more precise comprehension of the flow characteristics around their airfoils and accurate aerodynamic coefficients, particularly in the vicinity of the stall, where XFLR5 is recognized to be less reliable.

The meshing was done using the FLUENT meshing software. For a flow speed from 20 to 35 knots and $y+ = 1$, $\delta y = 3.4e^{-5}$ to $2e^{-5}$. These value were respected.

Furthermore, spatial merging has been confirmed for all airfoil designs. To illustrate, consider the R1 V5 Satori 3, which yielded the following results:

number of elements	138653	200150	288180
CL	0,1276	0,1272	0,1258
CD	0,0124	0,01245	0,0124
Finesse	10,2903	10,2169	10,1452

Table 2.4: R1 V5 Satori 3 results at 0° and 30 knots

Then, using the Richardson interpolation method [?]:

$$\begin{cases} p &= \frac{1}{\ln(r)} \frac{\ln(m_3 - m_2)}{\ln(m_2 - m_1)} \\ m^* &= \frac{m_3 - m_2 r^p}{1 - r^p} \end{cases} \quad (2.4)$$

(with m_i the results obtained for meshes with element sizes in a ratio r , m^* the asymptotic value and p the merging order)

We obtain :

	p	Asymptotic value	Required accuracy
CL	2,30	0,1247	e^{-2}
CD	2,73	0,0124	e^{-3}
Finesse	2,76	10,1452	e^0

Table 2.5: R1 V5 asymptotic results at 0° and 30 knots

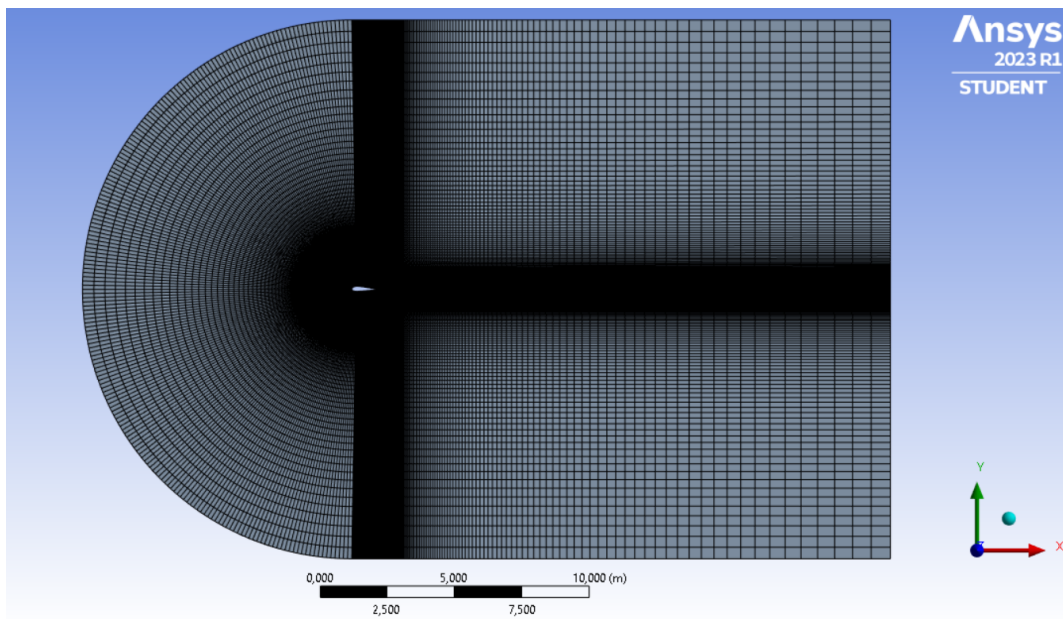


Figure 2.18: The global meshing under FLUENT

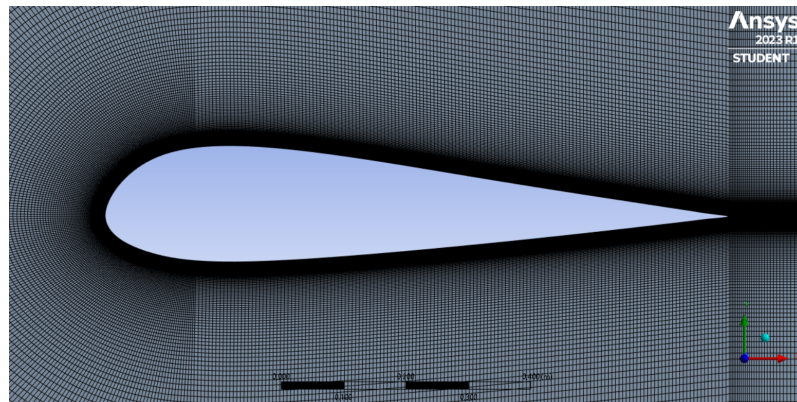


Figure 2.19: Zoom on the airfoil

2.6.2 The turbulence models

FLUENT offers various turbulence models.

Two models were tested to nuance the results :

- **Spalart-Allmaras :**

it is the only example of a transport equation model for ν_t used in the industry. This model is widely used in aerodynamics for various reasons: It is easy to numerically integrate, for attached flows, it produces results as good as zero-equation models, and for separated flows, it provides a much better description of the velocity field than zero-equation models. However, this model is too simple (a single equation) to be valid for a wide range of flows [?].

- **$k-\omega$ SST :**

The idea is to formulate a set of equations that converge towards the $k-\omega$ model near the wall and towards the $k-\epsilon$ model far from the walls. This model has been successfully applied in many configurations. It is currently one of the preferred models in the aerospace industry. $k-\omega$ provides better results than the standard $k-\epsilon$ model in adverse pressure gradient situations, allowing for a more accurate prediction of separation points. The $k-\epsilon$ and $k-\omega$ models use two scales, not just one, so the aim is to overcome the limitations of the Spalart-Allmaras model. However, this first-order linear model comes with several assumptions :

- instantaneity, where the deformation and turbulence history have no influence
- locality, where turbulence is influenced only by its immediate surroundings.
- materially simple environment
- linearity of the behavior law

It is understood, then, that first-order linear models cannot work in all situations [?].

The figures ?? and ?? compares the R1 V5 Satori 3 finesse plot at 35 knots with the two turbulence models. While the $k-\omega$ SST model is designed to provide more precise outcomes compared to the Spalart-Allmaras model, it introduces an elevated computational expense and an added difficulty in attaining spatial convergence. This is in contrast to the Spalart-Allmaras model, which generally converges toward a solution (that has spatially converged). Additionally, at low angles of attack, both models produce similar outcomes. It is only when encountering high angles of attack that noticeable disparities in results arise, reaching approximately 15% divergence.

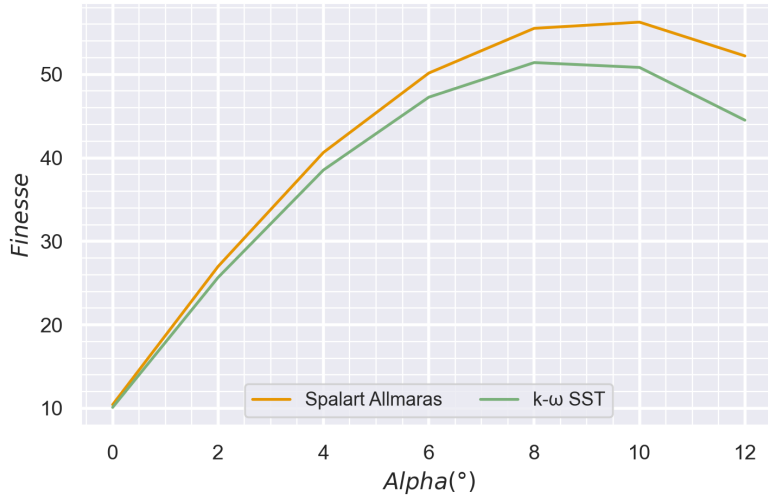


Figure 2.20: finesse against alpha

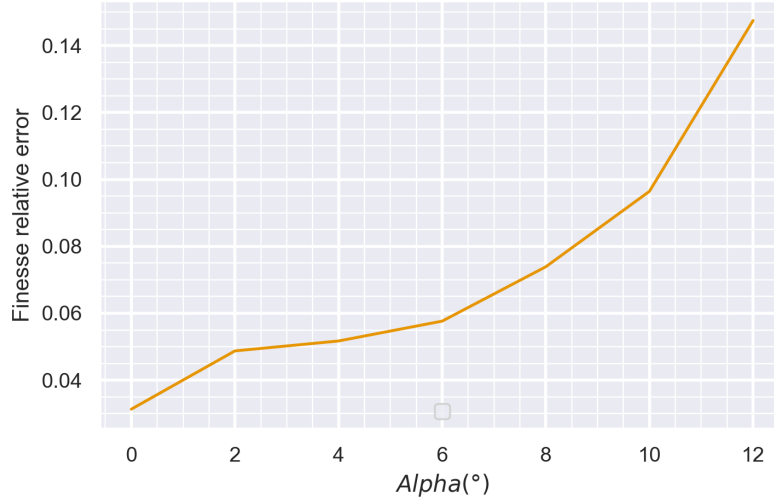


Figure 2.21: Finesse relative error against alpha

As a result, knowing the level of accuracy Ozone was looking for and the computational cost we could afford, **the Spalart-Allmaras model is the one we chose for our simulations.**

It's important to note that Ozone Kitesurf didn't seek highly precise results. Their primary objective was to gain insights into enhancing their existing airfoil while obtaining results that align with overall trends. Additionally, due to the computational limitations of my computer and the recognized influences of 3D effects, unsteadiness and fluid structure interactions, the pursuit of more precise results became less appealing.

2.6.3 The results

The following figure ?? shows the finesse plots for the R1 V5, R1 V5 Satori 3 and the VMG at 15 knots, the downwind conditions, and 35 knots, the upwind conditions.

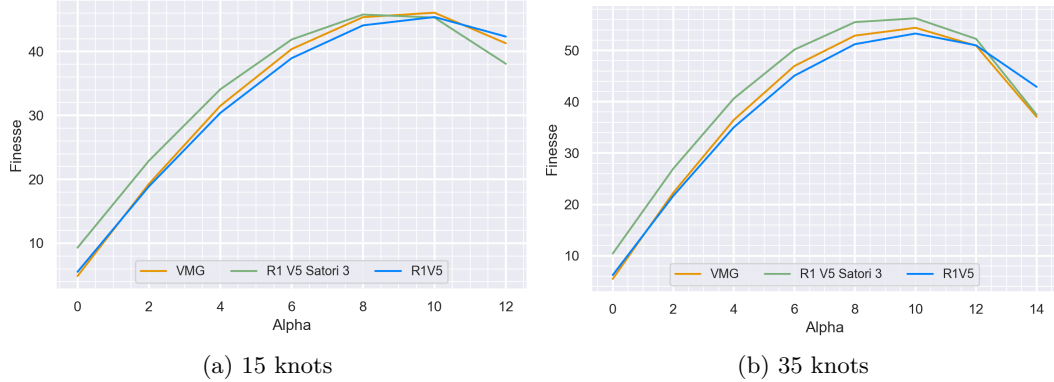


Figure 2.22: R1 V5, R1 V5 Satori 3 & VMG polars with FLUENT

These findings are rather promising, as we anticipate that the R1 V5 Satori3 will demonstrate enhanced performance in upwind conditions, particularly at low angles of attack, at 35 knots. Furthermore, in downwind scenarios, the R1 V5 Satori3 is projected to deliver favorable outcomes within the range of 5° to 8° angles of attack, but it is expected to experience a stall around 9-10°..

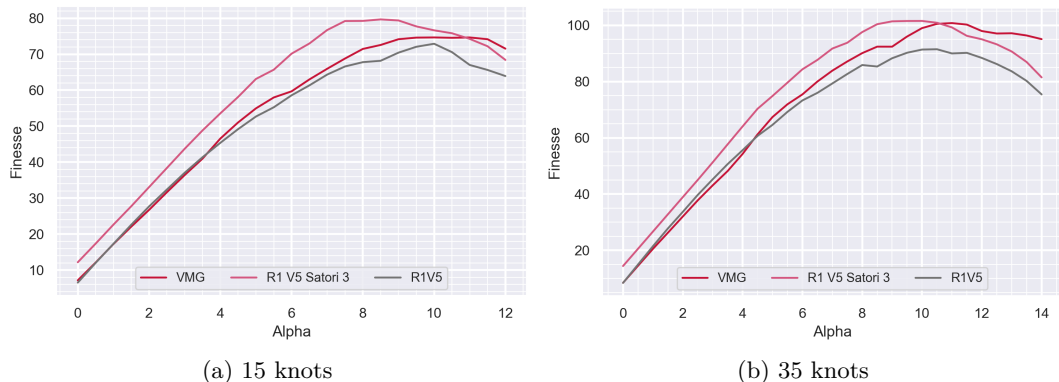


Figure 2.23: R1 V5, R1 V5 Satori 3 & VMG polars with XFLR5

We also recognize the necessity of utilizing Fluent for simulations to achieve greater result accuracy, particularly when approaching the stall at high angles of attack. In fact, XFLR5 tends to provide higher estimates for the finesse values but is valuable for quickly obtaining initial insights into the relative behaviors of airfoils.

The precision and cost-effectiveness of XFLR5 prompted, after extensive discussions with the paraglider design team, the initiation of a project to apply XFLR5's theories to simulate 3D effects and implement

an optimization algorithm. This project is the central focus of Chapter ??.

Consequently, we opted to initiate the development of a prototype for the R1 V5 Satori 3 and dispatch the kite to France for testing by the team riders to obtain their feedback on its performance.

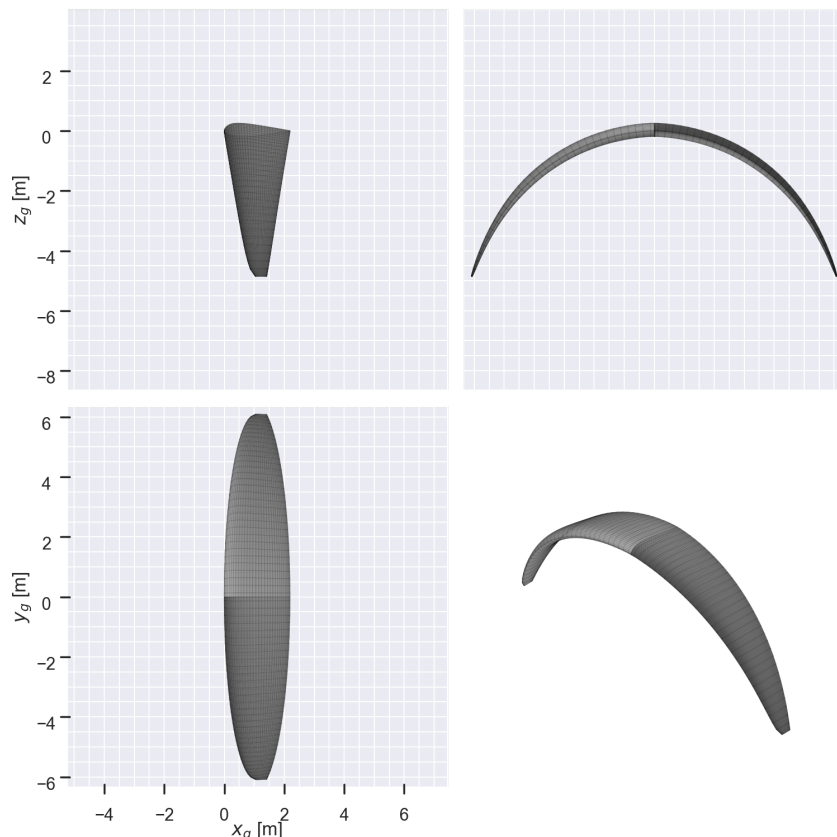


Figure 2.24: The R1 V5 Satori 3 3D view

2.6.4 The team rider feedbacks

After several hours of adjustments and continuous use of the kite prototype until it reached its "final" shape (bearing in mind that the fabrics relax during the initial hours of testing), the team riders achieved higher Velocity Made Good (VMG) values upwind and maintained greater tether tension when going downwind. They enthusiastically declared that this kite was the most high-performing one they had ever tested and expressed optimism about the future of the kite we were developing.

Moreover, the accuracy in predicting kite performance and the alignment between theory and practice reassured the Ozone's design team about using science to shape their future kites. In fact, the kite surfing community has only recently embraced scientific knowledge in fluid mechanics, and these results served as Ozone's initial evidence of the value that numerical simulations can bring to the company.

It's important to note that many kites have benefited from my research on kite aerodynamics. This is because not all kites aim for the same performance characteristics. For instance, the smaller version of the R1 V5, which has an area of $11m^2$ compared to the $21m^2$ kite discussed in this report, is used in stronger winds where the emphasis is not on exploiting the finesse of the kite (as the wind is already strong, and other factors like the pilot's skill or the performance of the submerged foil in the water are limiting), but rather on its stability. As a result, the entirety of the work developed in this report has contributed to the development of this kite, which serves very different objectives, but for which the contribution of scientific research has proven to be beneficial.

Once again, the feedback from the team riders during tests conducted on prototypes of these kites has proven to be in line with theory, and the kites developed in this manner have demonstrated higher performance than the existing ones.

Chapter 3

Optimization

Following the design of the R1 V5 Satori 3 and discussions with the Ozone paragliding design team, my attention turned to enhancing the performance of the kite. To achieve this, I collaborated with Fred Pieri, a paraglider designer, to develop an optimization algorithm. This algorithm, written in Python, makes use of the Aerosandbox library.

3.1 Aerosandbox

AeroSandbox[?] is a Python package that helps designing and optimizing aircrafts and other engineered systems. It is developed by Peter Sharpe, a graduate student studying aircraft design, multidisciplinary design optimization (MDO) and applied aerodynamics in MIT’s Department of Aeronautics and Astronautics.

At its heart, AeroSandbox is an optimization suite that combines the ease-of-use of familiar NumPy syntax with the power of modern automatic differentiation.

This automatic differentiation dramatically improves optimization performance on large problems: design problems with tens of thousands of decision variables solve in seconds on a laptop. AeroSandbox also comes with dozens of end-to-end-differentiable aerospace physics models, allowing users to simultaneously optimize an aircraft’s aerodynamics, structures, propulsion, mission trajectory, stability, and more.

3.1.1 The 2D aerodynamics

The 2D study uses "**NeuralFoil**". It is a tool for rapid aerodynamics analysis of airfoils, similar to Xfoil. Under the hood, NeuralFoil consists of physics-informed neural networks trained on tens of millions of Xfoil runs.

NeuralFoil is 10 times faster than Xfoil for a single analysis, and 1000 times faster for multipoint analysis, all with minimal loss in accuracy compared to Xfoil. Due to the wide variety of training data and the embedding of several physics-based invariants, this accuracy is seen even on out-of-sample airfoils (i.e., airfoils it wasn't trained on). [?]

It uses the 2D Panel Method. It is a computational technique used in aerodynamics to analyze the flow of fluids around two-dimensional objects. Here is a basic overview of how the 2D Panel Method works:

- Discretization: The surface of the object is divided into a series of panels, which are typically flat or slightly curved. These panels represent small segments of the object's surface.
- Vortex Elements: Each panel is then modeled as a vortex element that produces a velocity field at its position. These elements create a mathematical representation of how the fluid interacts with the object's surface.
- Superposition Principle: The key idea behind the Panel Method is that the total velocity at any point in the flow field is the sum of the velocities induced by all the panels. This is based on the principle of superposition, which allows you to add up the effects of individual panels to obtain the overall flow field.
- Kutta Condition: To ensure the accuracy of the method, a condition called the Kutta condition is applied at the trailing edge of the airfoil. This condition ensures that the flow separates smoothly from the trailing edge, which is physically realistic. (i.e. the flow circulation is conserved).
- Computational Solution: The method involves solving a system of linear equations to satisfy the boundary conditions at the surface of the object (normal velocity is equal to zero) and the Kutta condition at the trailing edge. Once this system is solved, it provides the velocity distribution around the object and can be used to calculate various aerodynamic parameters such as lift, drag, and pressure distribution.

The 2D Panel Method is especially useful for preliminary design and analysis. While it simplifies certain aspects of fluid dynamics, it can provide valuable insights and accurate results for many practical engineering applications.

3.1.2 The 3D aerodynamics

The 3D study uses the "**Vortex Lattice Method (VLM)**". It is a simplified mathematical approach that provides an approximate solution to the flow field around these objects. VLM is particularly useful for low-speed and subsonic aerodynamic analyses. Here is a basic overview of how the Vortex Lattice Method works:

- Discretization: The surface of the aerodynamic object is divided into a set of smaller, interconnected panels or segments. These panels are often assumed to be flat and have a constant strength vortex associated with them.
- Vortex Representation: Each panel generates a vortex, and these vortices collectively form a lattice that represents the overall geometry of the object. The strength and location of these vortices are determined based on the local flow conditions and geometry.
- Induced Velocities: The induced velocity at any point in the flow field, caused by all the vortices in the lattice, is calculated using mathematical equations. This induced velocity represents how the vortices affect the flow at a particular location.
- Boundary Conditions: The VLM considers boundary conditions, such as the no-slip condition at the object's surface and the freestream velocity far from the object.
- Solution for Aerodynamic Forces: Using the induced velocities and boundary conditions, the method calculates aerodynamic forces and moments on the object, such as lift, drag, and pitch moment.

It's important to note that the Vortex Lattice Method is a simplified approach and comes with certain limitations. For instance, it assumes steady, incompressible, and inviscid flow, neglecting turbulence effects and compressibility. As such, it is most suitable for preliminary design and analysis where a quick assessment of an object's aerodynamic characteristics is needed. Despite its simplifications, the Vortex Lattice Method has been widely used in the early stages of aircraft design and in the analysis of various aerodynamic configurations due to its efficiency and ability to provide valuable insights into the behavior of aerodynamic systems.

Note that Aerosandbox also offers to use the "**Lifting Line Theory**" (LLT). It is a more advanced analytical method than the VLM used to calculate the lift distribution along the span of a finite wing. It considers the variation in lift across the wing, taking into account the effects of downwash and induced drag. The LLT relies on the concept of vortex filaments to model the lift distribution and uses integral equations to determine the lift characteristics of the wing.

3.1.3 The geometry

The three main geometry objects used in this study are the "Airplane", the "Airfoil" and the "Kulfan Airfoil".

- The Airplane : it encapsulates the entire aircraft, comprising a collection of "Wing" objects, which constitute integral parts of the aircraft and are described by a list of sections, each featuring position, airfoil, twist angle, and chord parameters. Additionally, there is a list of "Fuselage" objects, which are also integral components of the aircraft and are associated with reference values.
- The Airfoil : It can be defined using either a set of coordinates or a NACA airfoil.
- The Kulfan Airfoil : the class shape transformation (CST) (Kulfan, 2008) is a popular airfoil parameterization [?]. It generates a shape using Bernstein polynomials to scale a class function, which is most often a base airfoil shape. They are built with "lower weights" (8 points), "upper weights" (8 points), "leading edge weight" (1 point) and a trailing edge thickness. This class has recently been added (August 2023) to Aerosandbox in order to allow 2D airfoil optimization.

3.1.4 The optimization

The Aerosandbox optimization part uses "**CasADi**", an open-source software tool for numerical optimization in general and optimal control (i.e. optimization involving differential equations) in particular [?]. It solves the optimization problems using CasADi with IPOPT backend.

"**Interior Point OPTimizer, pronounced I-P-Opt**" (IPOPT) is a software library for large scale nonlinear optimization of continuous systems [?]. IPOPT implements a **primal-dual interior point method**, and uses line searches based on Filter methods (Fletcher and Leyffer).

Primal-dual interior point method has the advantages of :

- efficiency for large-scale problems (can handle problems with a large number of variables and constraints)
- global convergence (can find solutions that are globally optimal or nearly optimal)
- handling inequality constraints
- well-suited for linear and convex problems
- predictable convergence behavior

but also has the disadvantages of :

- lack of flexibility (primarily designed for convex optimization problems)
- sensitivity to initial conditions
- computational cost
- limited support for non-smooth functions (functions that have continuous derivatives of all orders)

Consequently, although certain drawbacks, such as computational cost and sensitivity to initial conditions, were encountered in its utilization, the primal-dual interior point method continued to prove highly suitable for this specific application.

3.2 2D optimization

The 2D optimization algorithm was developed with the objective of improving the airfoil profile beyond that of the R1 V5 Satori 3, starting with the same base profile and introducing variations to the four parameters on the upper surface. The decision was made to retain the lower surface of the R1 V5 Satori 3 since it exhibited a "realistic" shape that yielded favorable results. The optimization program in Python incorporated the following conditions :

- The C_l must stay superior to the initial airfoil ones at few angles of attack ($0^\circ, 2.5^\circ, 5^\circ, 7.5^\circ, 10^\circ, 12.5^\circ, 15^\circ$)
- The trailing edge angle must be superior or equal to the initial airfoil one
- The local thickness must stay positive
- The $\frac{d^2}{dx^2}$ of the local thickness must stay negative
- The $\frac{d^2}{dx^2}$ of the local camber must stay negative
- The $\frac{d}{dx}$ of the upper coordinates must stay negative after the upper apex
- The $\frac{d}{dx}$ of the lower coordinates must stay positive after the lower apex
- the maximum thickness must be superior or equal to 19% of the chord

The following result was reached after 4 secondees :

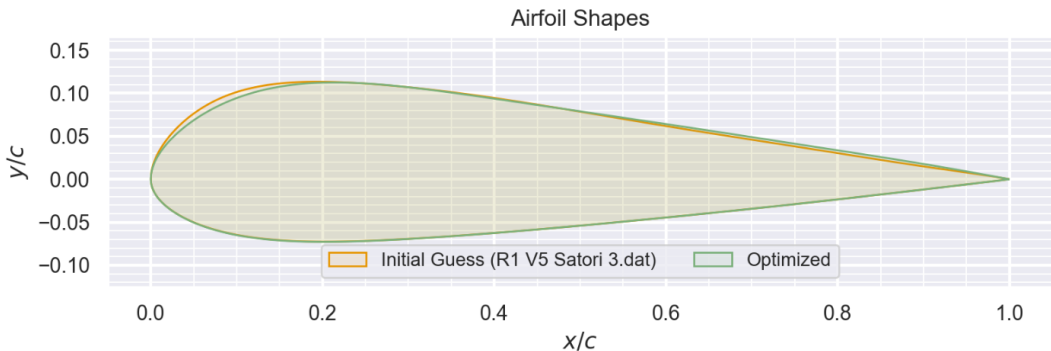


Figure 3.1: Comparison between the Initial Guess Airfoil and the Optimized Airfoil

We can see on the figure ?? that the algorithm put the apex slightly backward to increase the airfoil finesse.

As a results, simulations with Fluent were run in order to validate the airfoil before starting a new prototype :

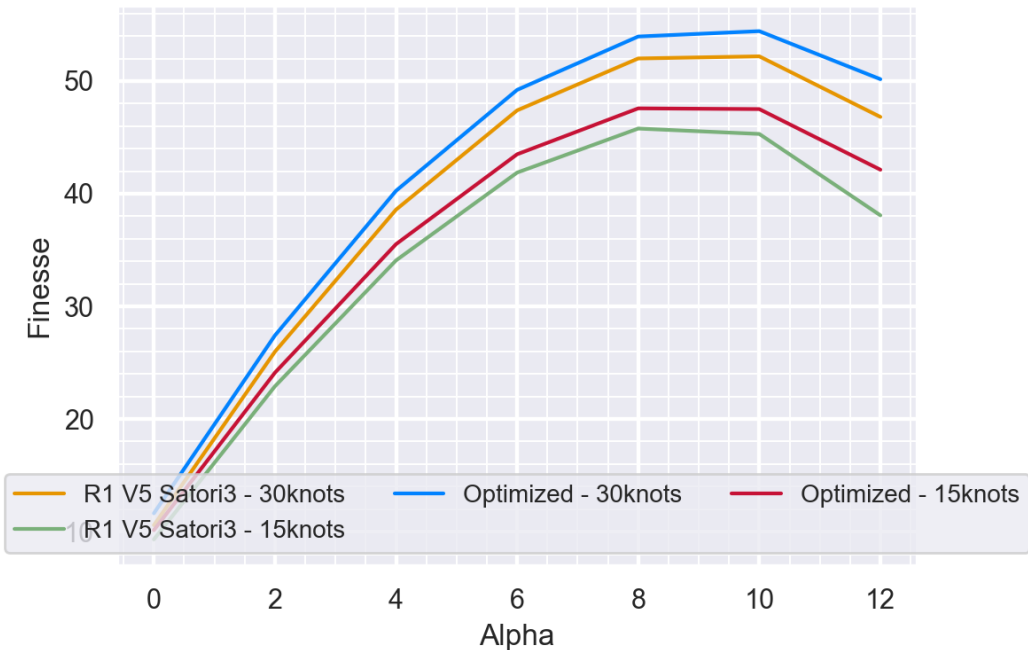


Figure 3.2: Finesses of the R1 V5 Satori3 and the optimized airfoils (FLUENT)

Figure ?? suggests that the theoretically optimized airfoil should outperform the R1 V5 Satori 3.

It's worth noting that 3D effects and actual testing may reveal unforeseen factors that could potentially impact the performance of the optimized profile. However, at

this stage, there is confidence that this airfoil is an improvement over the current airfoil under evaluation.

3.3 3D optimization

An alternative approach to enhance the performance of the R1 involves optimizing 3D parameters. I initially concentrated on optimizing the twist distribution along the span and subsequently extended the optimization to the wing's planform.

The primary challenge associated with 3D optimization lies in the computational cost. In practice, even though VLM simulations might not appear significantly more complex at first glance, the algorithm must address 33 variables in 3D (corresponding to 33 sections along the wing's span) as opposed to the 10 variables used in 2D (related to Kulfan airfoil parameters).

This elevated level of complexity may result in outcomes that fail to converge, an excessive number of iterations, or a shortage of available computer memory space.

Additionally, the need for spatial discretization along both the wing's span and its chord required an evaluation of spatial convergence when employing the vortex lattice method before initiating the optimization of the twist distribution along the span.

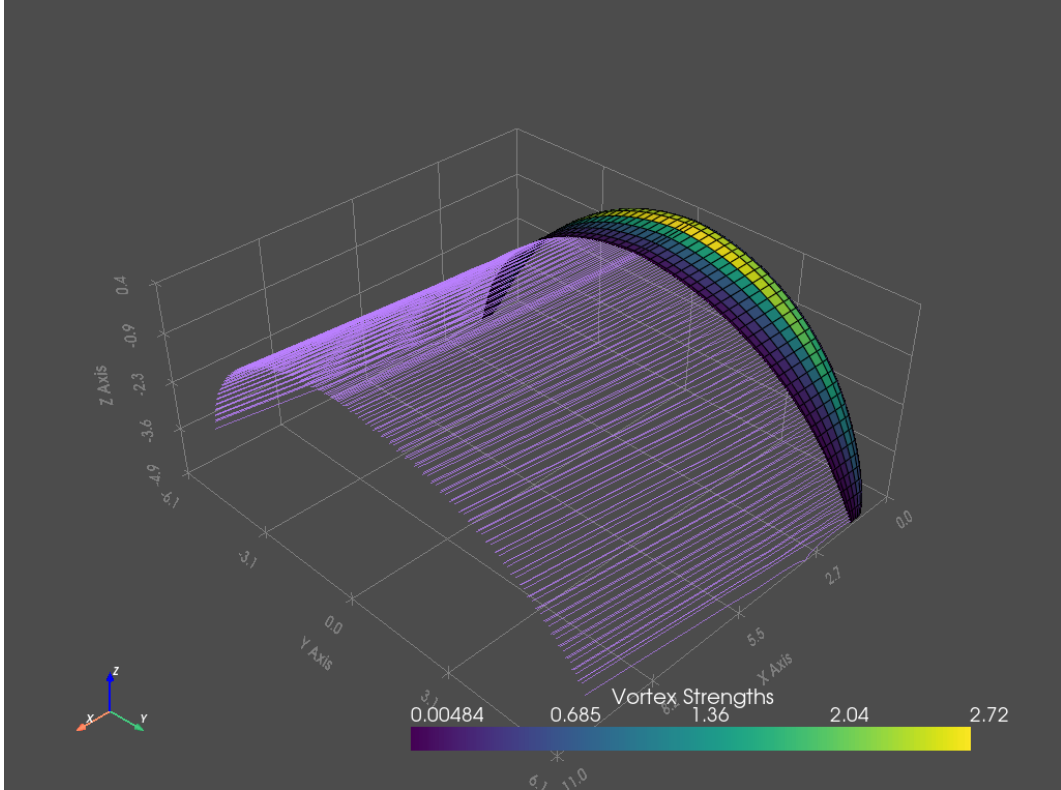


Figure 3.3: Draw of a VLM simulation on the R1 V5 Satori 3

3.3.1 The spatial convergence of the VLM simulations

Aerosandbox offers to discretize along the chord via "*chordwise_resolution*" and along the span via "*spanwise_resolution*", two parameters of the VLM function. Note that *spanwise_resolution* is the number of element aerosandbox considers between two sections of the wings. As the wing is defined with 33 sections, a *spanwise_resolution* of k means $33 * k$ elements along the span.

Therefore, VLM simulations have been run for different values of these very two parameters in order to find the values for which the simulations can be considered to have sufficiently converged to their asymptotic values.

Note that results in terms of relative error don't change with the speed or the aerodynamic coefficient we calculate.

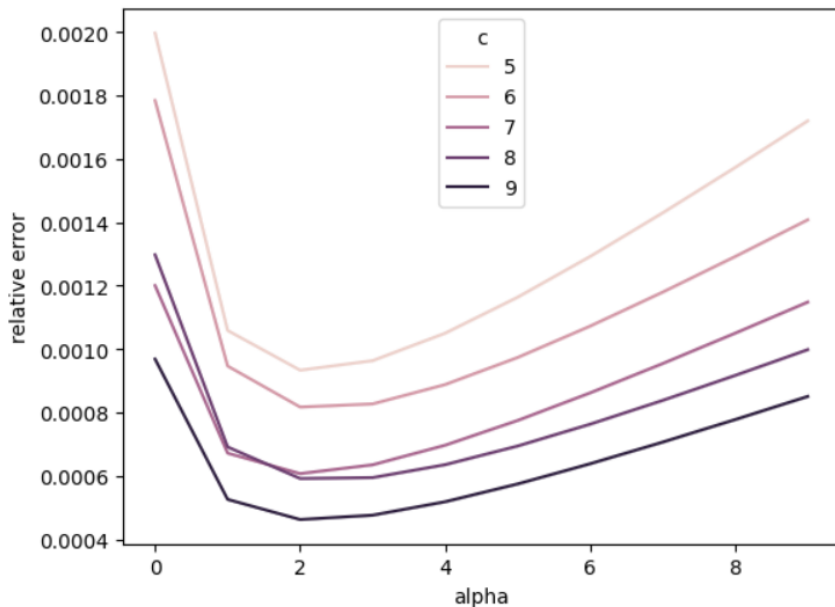
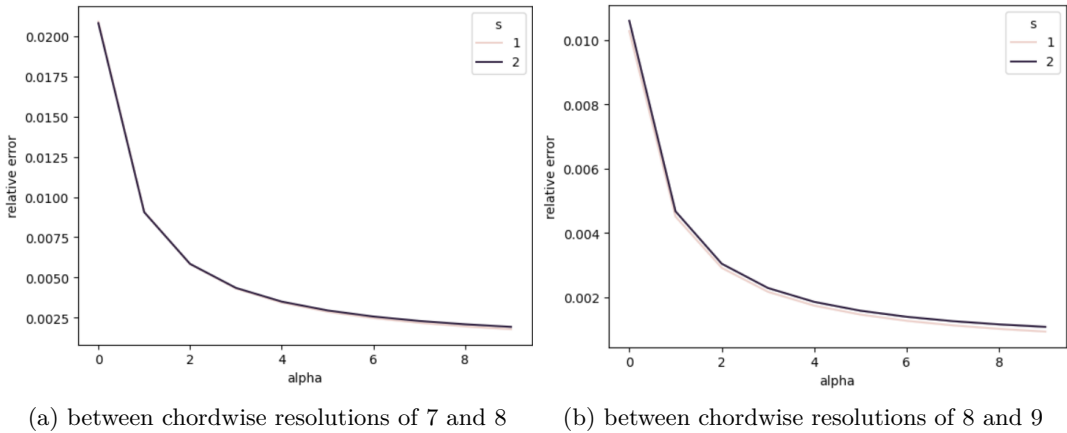


Figure 3.4: Relative error in lift force between a spanwise resolution of 1 and 2

The figure ?? shows that choosing *spanwise_resolution* = 1 is enough to consider the simulation to have spatially converged. Note that in figures ?? and ?? "c" is the *chordwise_resolution* parameter and "s" is the *spanwise_resolution* parameter.



(a) between chordwise resolutions of 7 and 8 (b) between chordwise resolutions of 8 and 9

Figure 3.5: Relative error in lift force

The figure ?? shows that we can already consider the VLM simulations to have converged for *chordwise_resolution* = 8. This *chordwise_resolution* value is a good compromise between computational cost and accuracy.

As a consequence, the following parameters have been selected for VLM simulations using Aerosandbox to achieve spatial convergence while minimizing computational costs :

- *chordwise_resolution* = 8
- *spanwise_resolution* = 1

3.3.2 The twist optimization

The twist optimization is intended to address the issue of reduced finesse at high angles of attack and during downwind maneuvers. Based on feedback from team riders, the existing kites do not exhibit sufficient forward flight characteristics, resulting in riders experiencing a lack of tension in the lines during their rides. Furthermore, Benoit Augier, a Ph.D. expert in fluid mechanics at the Marine Hydrodynamic Laboratory in Brest, who is currently collaborating with the French kitesurfing team for the Olympic Games, suggests that there is still room for reducing kite drag under these conditions changing the kite twist or its planform.

However, it encounters a challenge in terms of computational complexity. Unlike 2D optimizations, which typically take about 10 minutes to complete, the twist optimization algorithm requires several hours to run. If I lack the resources required to conduct simulations until we have a precise law that defines the optimal kite twist at various angles of attack, I can, however, run a simulation at a single angle of attack to obtain an initial glimpse of what such a twist profile might look like.

Therefore, I executed the optimization algorithm at a 9° angle of attack and a wind speed of 20 knots, under the following conditions :

- The kite should support a load of 150 kg
- The $\frac{d}{dz}$ of the twist cannot exceed $3^\circ/\text{section}$ (a physical constraint that ensures manufacturability)

The algorithm required 62 minutes to complete.

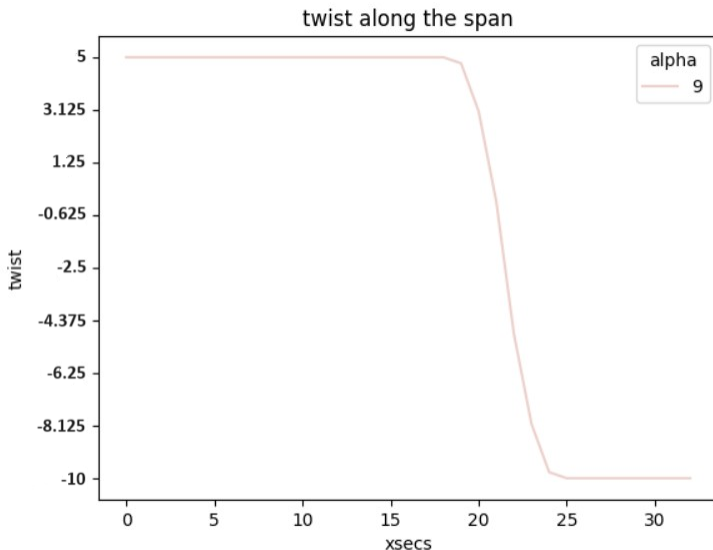


Figure 3.6: The twist distribution along the wing's span that minimizes drag at a 9° angle of attack during downwind conditions (at 20 knots)

The figure ?? indicates that the algorithm strives to distribute the load evenly across the kite's middle section and minimize drag resulting from tip vortices.

Currently, these results haven't been utilized by Ozone kitesurf due to the tight deadlines the brand faces for submitting the kite sail design for the 2028 Olympic Games. However, this 3D optimization algorithm could prove beneficial for the brand if tested on their future prototypes, offering an alternative means of improving kites performances.

Furthermore, the Ozone paraglider design team is already engaged in this project, and their upcoming paraglider design may benefit from the use of this algorithm.

While planform optimization has also been implemented, it is computationally intensive and strains the capabilities of my computer. With access to more powerful computing resources, both planform and twist optimizations could be conducted simultaneously, providing the design team with a kite that fully harnesses the potential of its airfoil.

3.3.3 The equilibrium of moments

Another algorithm has been employed for the prediction of the kite's position within the wind window. By leveraging the knowledge of the bar position set by the athlete

and applying the principles of moment equilibrium (minimizing the absolute value of the moment with an optimization algorithm) around the athlete between the kite's aerodynamic forces and the drag in the lines, we were able to compute the kite's angle of attack.

Remarkably, this algorithm achieved a prediction that had previously remained elusive for Ozone and, as far as my research indicates, for anyone in the kitesurfing community: the angle of attack of a kite and its positioning in the wind window, relying solely on the kite's aerodynamic properties without knowledge of water foil drag or athlete drag.

Consequently, the algorithm effectively validated the data in Table ?? and stands as a robust tool for Ozone to forecast kite flight conditions based on the athlete's speed.

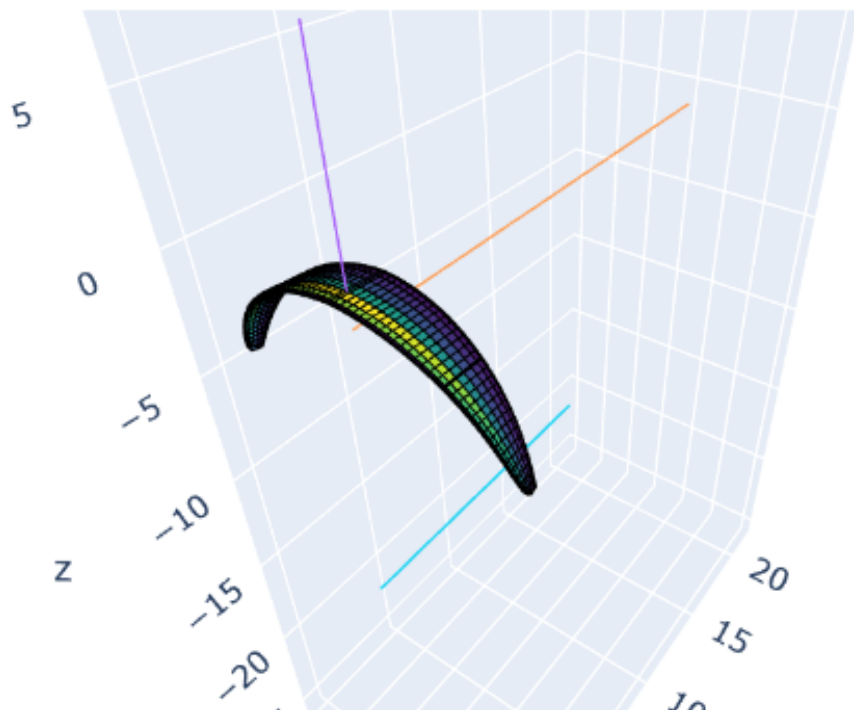


Figure 3.7: An illustration depicting the equilibrium of moments on the athlete (25 meters under the kite) (with rescaled forces)

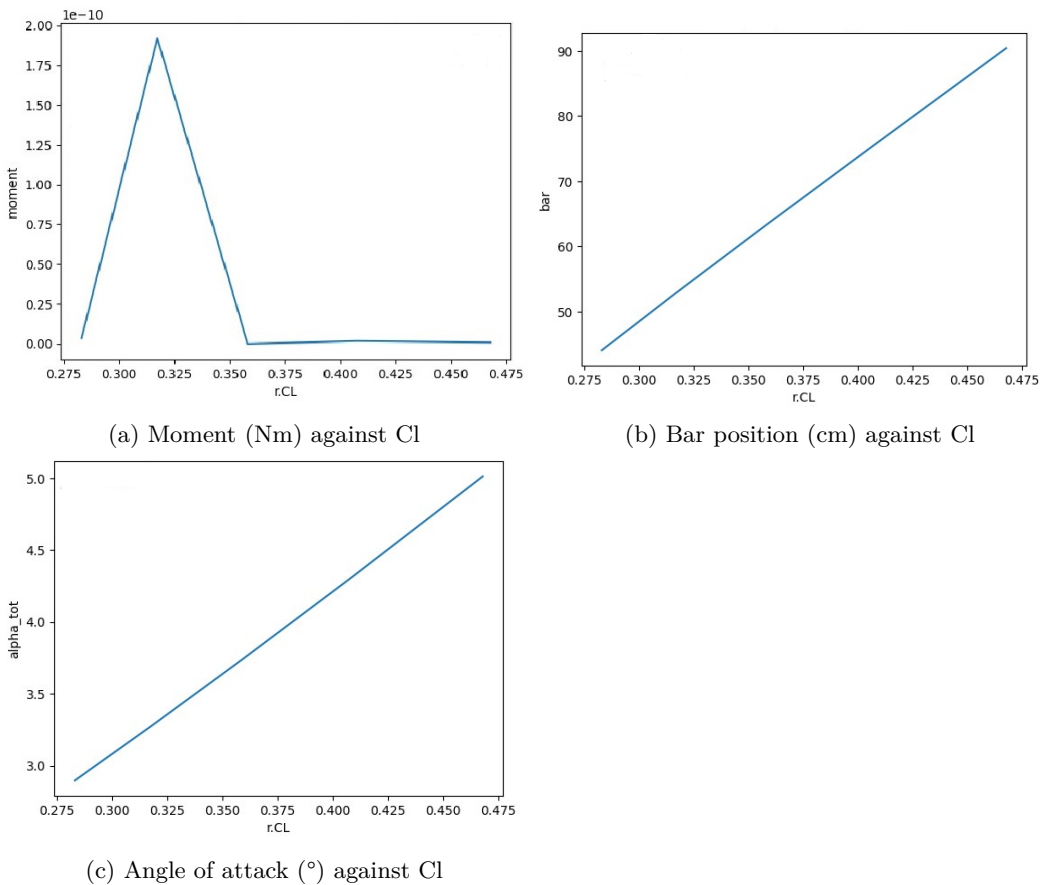


Figure 3.8: Plots at 35 knots (Upwind conditions)

The information presented in Figure ?? clearly indicates that, under upwind conditions, and with an offset applied to the bar position to attain the actual kite deformation, the kite's angle of attack falls within the range of 0° to 5° , aligning with the predictions detailed in Table ??.

Chapter 4

Stability

During discussions with the team riders testing the new prototypes, it became evident that another critical phenomenon significantly impacted kite performance.

In general, when a rider is moving downwind, they prefer the kite to exhibit a strong forward impulse, causing it to move deep into the wind window, even if the athlete maintains bar tension. Conversely, when a rider is heading upwind, the kite naturally wants to surge forward, especially when it flies at high Reynolds numbers and low angles of attack. But in contrast to downwind conditions, when the kite surges forward while going upwind, it tends to move out of the wind window. When the brakes halt the kite's forward movement after "shooting" forward, if the kite continues to progress forward due to a negative pitching moment, it may collapse.

The manner in which a kite behaves when coming to a stop after moving forward, and how it attains its moment equilibrium, is frequently referred to as "**stability**" in kitesurfing. An unstable kite is one that continues to move forward even after the brakes have stopped it during a "shoot" (dynamic forward flight); it is a kite that proves challenging, and at times impossible, to control because it **collapses**.



Figure 4.1: Picture of a paraglider pilot experiencing a front collapse

4.1 The aerodynamic definition of stability

This issue of stability is well known in the paragliding world. As the physics is quite the same and the stakes are much higher, the Ozone paragliders designers have been able to help me translating the notion of stability in terms of aerodynamics.

Contrary to the popular belief, a kite doesn't collapse when its incidence becomes negative, but before. "the collapse comes from the fact that the A lines bend more than the B lines under their own aerodynamic drag", according to the Ozone paraglider designers.

Assuming that A lines drag and B lines drag are the same, for the kite to be stable, the tension in the A lines must be higher than the tension in the B lines. It also means that the aerodynamic force component collinear with the lines must be higher in the A lines than the B lines.

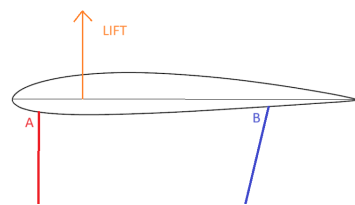


Figure 4.2: A lines, B lines and lift on a kite airfoil

Assuming that A lines and B lines are parallels near their towpoints (where the kite lines are tied) and considering a LIFT that represents the aerodynamic force component collinear with the lines, we have :

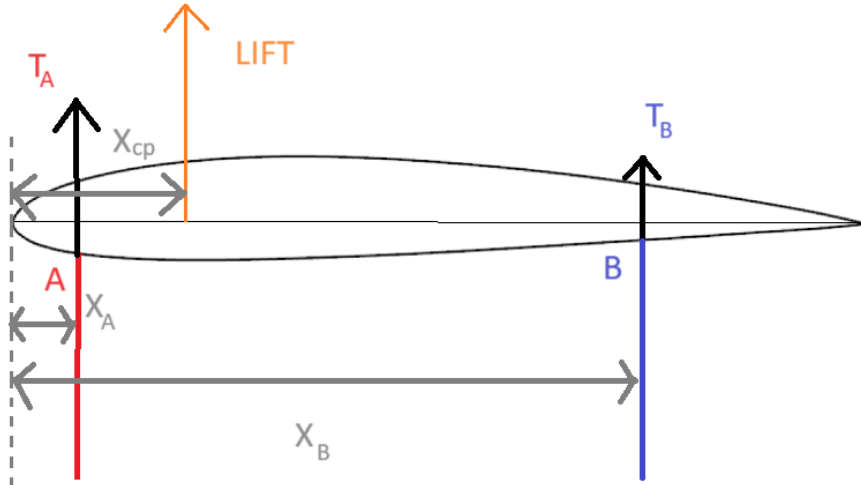


Figure 4.3: A and B tensions on a kite airfoil

$$\begin{cases} T_A = LIFT \frac{X_B - X_{cp}}{X_B - X_A} \\ T_B = LIFT \frac{X_{cp} - X_A}{X_B - X_A} \end{cases} \quad (4.1)$$

$$T_A \geq T_B M_S \iff X_{cp} \leq \frac{X_B + X_A}{2M_S} \quad (4.2)$$

With M_S the static margin.

As a result, we understand here that the aerodynamic force position along the chord X_{cp} is a measure of the kite stability.

4.2 The theoretical existing kite stability

To corroborate the aerodynamic concept of stability as outlined in section ??, a stability graph denoted as $X_{cp}(C_L)$ was generated for each kite subjected to testing by our team riders.

It is known that :

- The R1 V4 is a very stable kite
- The R1 V5 is more stable than the VMG (but less performant)
- The Vmg is close to the limit of stability
- The R1 V5 Satori3 is more unstable than the VMG but still stable (if well trimmed)

- "Limit stability" refers to an airfoil that has undergone testing by Ozone paraglider team pilots and is regarded as the threshold of stability. In this context, it serves as an initial reference.

Running 2D simulations on these kites airfoils with aerosandbox, the following results have been obtained at 18knots and angles of attack from 2° to 13° :

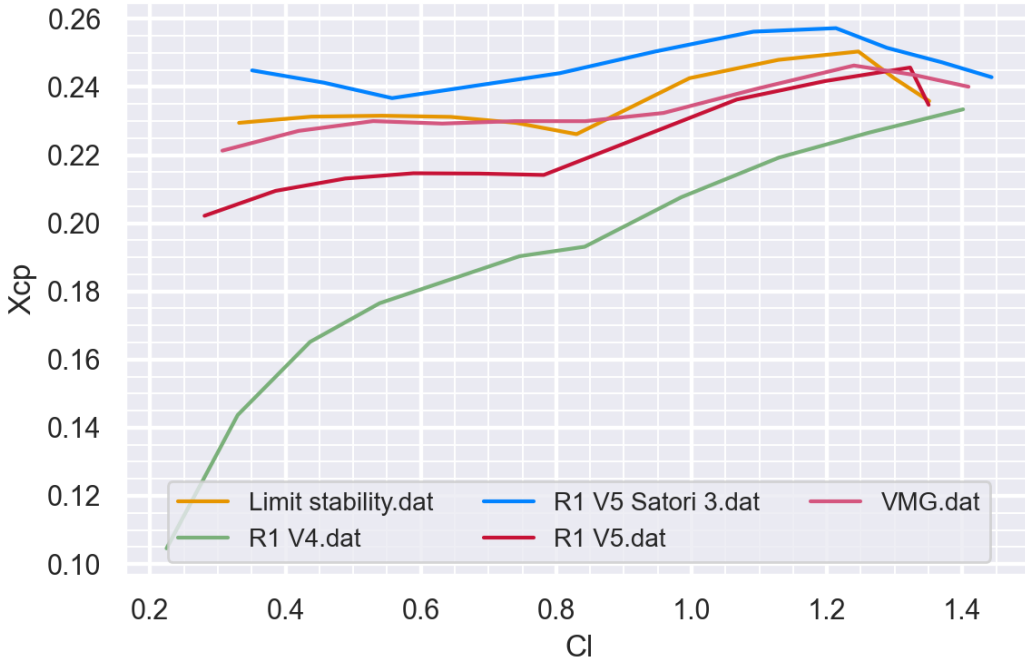


Figure 4.4: X_{Cp} plot against C_L

It's worth noting that since stability is already noticeable on the beach, when the athlete's speed is at 0 knots, the value of 18 knots (wind speed) serves as a suitable benchmark for comparison with the feedback from the team riders. This is particularly pertinent because when they are stationary on the beach, there are fewer external factors that could affect the results compared to when they are actively riding out at sea.

The figure ?? shows that the aerodynamic definition of a kite stability established in ?? is in line with the pro kitesurfers' feelings.

Moreover, the figure ?? shows two characteristics that seem to be sources of instability :

- **high X_{Cp} values**
- **A negative slope of the X_{Cp} curve at low angles of attack**

Furthermore, it can be deduced from equation ??, taking into account that for the present kites $X_A = 0.07$ and $X_B = 0.63$, and considering that $X_{cp} = 0.26$ serves

as the stability threshold as depicted in figure ??:

$$\underline{M_S} = 1.35$$

4.3 The add of stability in the airfoil optimization

Taking the stability matter into account, the next step was to generate an optimized airfoil, like in ??, with the add of a stability constraint in the algorithm.

It is assumed that the more the airfoil is optimized, the more unstable it becomes. This is something we can observe on the prototypes we test but also regarding of the figure ??.

Furthermore, figure ?? illustrates that the presently optimized airfoil, discussed in Section ??, exhibited excessive instability, making it unsuitable for use in the upcoming prototype.

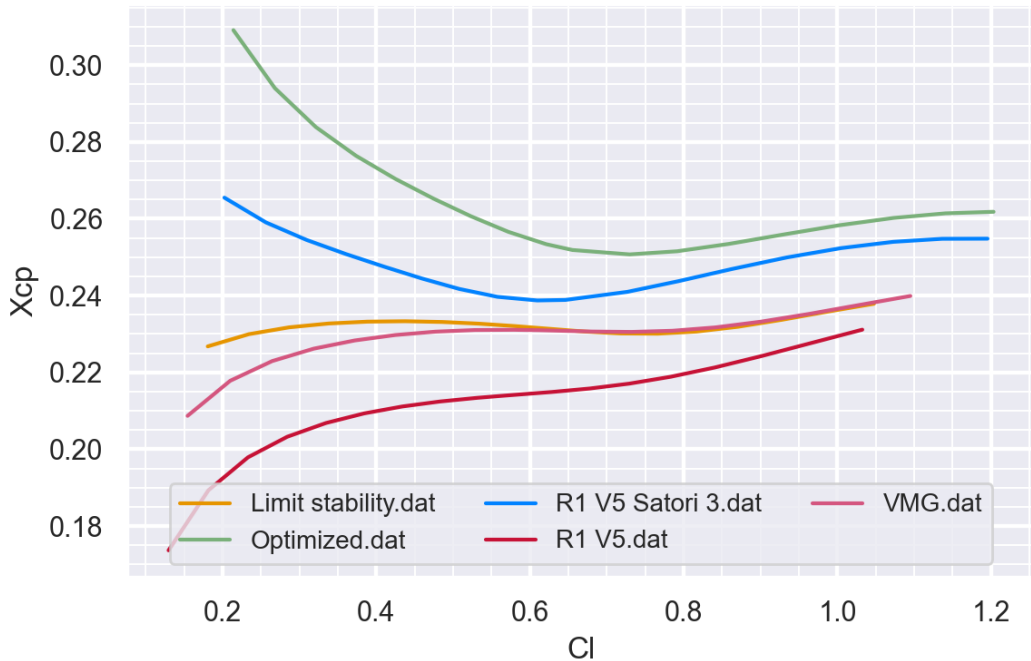


Figure 4.5: Stability comparison between the existing airfoils and the optimized one

Consequently, the optimization algorithm was adapted to seek an airfoil that lies on the brink of instability while delivering the best possible performance, specifically by maximizing its finesse.

Nonetheless, the Ozone design team opted to delay the adjustment of the value of M_S , referenced in Section ??, until the team riders had the opportunity to test the optimized airfoil identified in Section ???. Given that the stability constraint imposes significant limitations on the optimization algorithm, it was prudent to first

confirm that the current optimized airfoil exhibited instability. However, the team riders have not yet conducted tests on the optimized profile, and the value of M_S remains to be verified.

Furthermore, this phase in airfoil design underscored the significance of the initial guess airfoil in the optimization process. It became evident that the algorithm encountered difficulties in reversing the stability graph of an airfoil. In fact, the sign of the slope in the X_{cp} plot at low Cl values would remain unaltered during the optimization process. This implies that starting with an unstable airfoil as the initial guess would not lead to a stable optimized airfoil.

Chapter 5

Conclusions

The primary objective of this internship was to develop Ozone's next-generation R1 formula kite for the 2028 Olympic Games. This endeavor began by utilizing the previous R1 kite version, R1 V4/V5, and the FlySurfer brand's VMG, known for its exceptional performance, as reference points. The overarching goal was to create the most high-performance kite possible for formula kite racing. Additionally, this internship aimed to introduce Ozone to a scientific approach to kite design, incorporating aerodynamic coefficients. Understanding the principles governing kite flight and translating these insights into aerodynamic characteristics proved beneficial in the pursuit of a more high-performance kite.

The process commenced with a comparative analysis of existing airfoils. This analysis allowed the experienced design team to discern the specific differences that contributed to the superior performance of the VMG kite compared to the R1 V4/V5. Subsequently, I employed Fluent simulations to meticulously design a new iteration of the R1 kite, resulting in the R1 V5 Satori 3 prototype. This prototype underwent extensive testing by our team riders and demonstrated superior performance compared to the VMG kite.

Furthermore, an optimization algorithm was developed using the Python library Aerosandbox. This algorithm was designed based on the same principles as XFLR5, serving as a preliminary airfoil design tool. It began with the R1 V5 Satori 3 as an initial reference and iteratively converged towards an even higher-performing kite design. Additionally, a 3D optimization algorithm was developed, building upon the principles of the 2D version but incorporating 3D effects and optimizing 3D

parameters. While the 3D optimization program has not yet been utilized by Ozone, both algorithms offer valuable tools for the brand's future kite design endeavors.

The 2D optimization program has been employed to design several kites, not limited to the R1 formula kite, which was the focus of this internship. This demonstrates its flexibility in optimizing the parameters as desired by the designer. Furthermore, the 3D optimization program is being utilized by the paraglider design team on their considerably more powerful computers than mine. Should both teams, the paraglider design team and the kitesurf design team, collaborate and utilize this algorithm on their high-performance computers, it has the potential to yield significant benefits for the development of future Ozone kite versions.

In summary, the outcomes of this internship have played a pivotal role in assisting the Ozone team in crafting their next-generation formula kite, the R1 V5, slated for use in the 2028 Olympics. Furthermore, the implementation of optimization algorithms and the calculation of aerodynamic coefficients provide Ozone with a solid foundation for their future kite designs.

Ultimately, this internship exposed me to the real-world challenges that engineers encounter within a company. The constraints of limited budgets also result in restricted simulation options, and addressing this challenge has encouraged me to explore creative and ingenious solutions. Additionally, the human aspects of water sports, including the sensations experienced by athletes when riding a formula kite, introduced an engineering dimension that I had not previously encountered but proved to be highly beneficial in expanding my open-mindedness.

References

- [1] Joel A E Andersson, Joris Gillis, Greg Horn, James B Rawlings, and Moritz Diehl. CasADi – A software framework for nonlinear optimization and optimal control. *Mathematical Programming Computation*, 2018. [Cited on page 31]
- [2] The International Kiteboarding Association. Registered series production kites 2020-2024. Available at <https://www.formulakite.org/equipment/eligible-equipment/kites-2020-2024>, May 2021. (Last access the 23/07/2023). [Cited on page 7]
- [3] International Olympic Committee. Kiteboarding set for lift-off at paris 2024. Available at <https://olympics.com/en/news/kiteboarding-set-for-lift-off-at-paris-2024>, 2023. (Last access the 22/07/2023). [Cited on page 6]
- [4] André Deperrois. Why does an airfoil drag: the viscous problem. Available at <http://www.xflr5.tech/docs/>, 2019. (Last access the 22/08/2023). [Cited on page 15]
- [5] Jérémie Gressier. *Introduction à la Simulation Numérique*. PhD thesis, ISAE-SUPAERO, 10 Av. Edouard Belin, 31400 Toulouse, November 2016. [Cited on page 21]
- [6] Kristen Kallstrom. *Exploring Airfoil Table Generation using XFOIL and OVERFLOW*. PhD thesis, NASA Ames Research Center, Moffett Field, CA, 94035, january 2022. [Cited on pages 15 and 17]
- [7] Brenda M. Kulfan. *A Universal Parametric Geometry Representation Method – “CST”*. PhD thesis, 45th AIAA Aerospace Sciences Meeting and Exhibit, Reno, Nevada, January 2007. [Cited on page 31]
- [8] Ozone Kitesurf Ltd. About ozone. Available at <https://ozonekites.com/about-ozone/>, 2023. (Last access the 22/07/2023). [Cited on page 5]
- [9] Remi Manceau. *Modélisation de la turbulence pour la CFD*. PhD thesis, ENS-GTI, street Jules Ferry, 64000 Pau, July 2023. [Cited on pages 22 and 23]
- [10] Guilhem Bles Jean-Baptiste Leroux Christian Jochum Yves Parlier Richard Leloup, Kostia Roncin. *Use of kites as an auxiliary propulsion method*

for ships: estimation of kite aerodynamic characteristics and performance prediction for a sailboat and a merchant vessel. PhD thesis, ISAE-SUPAERO, Toulouse, November 2012. [Cited on page 9]

- [11] Peter Sharpe. NeuralFoil: An airfoil aerodynamics analysis tool using physics-informed machine learning. <https://github.com/peterdsharpe/NeuralFoil>, 2023. [Cited on page 29]
- [12] Peter D. Sharpe. Aerosandbox: A differentiable framework for aircraft design optimization. Master's thesis, Massachusetts Institute of Technology, 2021. [Cited on page 28]
- [13] Andreas Wächter Stefan Vigerske. Ipopt documentation. <https://coin-or.github.io/Ipopt/>, 2023. [Cited on page 31]